

ANALYSIS OF THIN FILM FLOW OF OLDROYD-B NANOFLUID  
IN AN OSCILLATING INCLINED BELT WITH CONVECTIVE BOUNDARY CONDITIONS

\*DEBASISH DEY AND ARDHENDU SEKHAR KHOUND

Department of Mathematics,  
Dibrugarh University, Dibrugarh-786 004, Assam, India.

(Received On: 10-04-18; Revised & Accepted On: 29-06-18)

ABSTRACT

*The time-dependent thin film flow problem of visco-elastic fluid consisting of nano-sized particles through an inclined belt has been studied in presence of transverse magnetic field. The constitutive equation of fluid flow is characterized by Oldroyd-B fluid model bearing rheological parameters: relaxation parameter and retardation parameter. The lower surface of the belt is oscillating about a non-zero constant mean velocity  $U$ . Outer surface is characterized by convection-conduction and convection-diffusion boundary conditions. Governing equations of motion are solved analytically by using perturbation scheme. Closed form solutions for velocity profiles, shearing stress, temperature and concentration fields are constructed. Results are discussed graphically for various values of flow parameters involved in the solution with a special emphasis are given on effects of relaxation and retardation parameters.*

**Keywords:** Relaxation and retardation, Oldroyd-B fluid model, Nanofluid, Perturbation scheme, Shearing stress.

1. INTRODUCTION

In recent time, the visco-elastic fluid flow has attracted many scientists and researchers because of its uses in various industries such as polymer solution, suspension, paints, cosmetic products etc. Oldroyd [1, 2] proposed a model to study the flow pattern of visco-elastic fluid and is named as Oldroyd model. The mechanism of two rheological parameters relaxation time and retardation time in the Oldroyd fluid model has attracted many researchers as it can study the visco-elastic fluid motion in more generalized way (Dey [3, 4, 5], Dey and Khound [6, 7]). Viscoelastic fluid flow applications may be seen in various polymer industries, blood flow etc. In blood circulatory system, blood's elasticity restores an amount of energy, its viscosity dissipates mechanical energy into heat and the remaining part is responsible for the movement of blood [8]. The constitutive equation of Oldroyd fluid model is given by

$$\sigma_{ij} = -p\delta_{ij} + \tau_{ij}$$
$$\left(1 + \lambda_1 \frac{d}{dt}\right) \tau_{ij} = 2\mu \left(1 + \lambda_2 \frac{d}{dt}\right) e_{ij} \quad (1.1)$$

where,  $\sigma_{ij}$  is stress tensor,  $p$  hydrostatic pressure,  $\delta_{ij}$  kronecker delta,  $\tau_{ij}$  viscous-stress tensor,  $\lambda_1$  relaxation time,  $\lambda_2$  retardation time,  $\mu$  co-efficient of viscosity,  $e_{ij}$  is strain tensor and  $\frac{d}{dt}$  is material derivative. ( $\lambda_1 = 0, \lambda_2 = 0$ ) characterizes Newtonian fluid, ( $\lambda_1 = 0, \lambda_2 > 0$ ) characterizes Second-grade fluid, ( $\lambda_1 = 0, \lambda_2 < 0$ ) characterizes Walters liquid and ( $\lambda_1 \neq 0, \lambda_2 = 0$ ) represents the Maxwell fluid model.

Nano fluids are suspensions of nano particles in fluids. Mechanism of nano-fluid can be utilized where heat transfer enhancement is dominant as in many industrial applications, nuclear reactors, transportation, electronics as well as biomedicine and food (Wong and Leon [9]). Singh and Dikshit [10] have studied the hydro-magnetic flow past a continuously moving semi-infinite plate for large suction using similarity solution. Nield and Kuznetsov [11] have analysed the Cheng–Minkowycz problem for natural convective boundary-layer flow in a porous medium saturated by a nano fluid. Thermal instability in a porous medium layer saturated by a nano fluid has been investigated by Kuznetsov and Nield [12]. Chamkha *et.al* [13] have studied the non-similar solution for natural convective boundary layer flow over a sphere embedded in a porous medium saturated with a nanofluid. Shah *et.al* [14] have investigated the optimal homotopy asymptotic method for thin film flows of a third grade fluid. Natural convection boundary layer flow over a truncated cone in a porous medium saturated by a nanofluid has been analysed by Cheng [15] using cubic spline collocation method. Shahid *et.al* [16] have formulated the exact solution for motion of an Oldroyd-B fluid over an

**Corresponding Author: Ardhendu Sekhar Khound**  
**Department of Mathematics, Dibrugarh University, Dibrugarh-786 004, Assam, India.**

infinite flat plate that applies an oscillating shear stress to the fluid using Laplace and Fourier transforms. MHD Thin film flows of a third grade fluid on a vertical belt with slip boundary conditions have been investigated by Gul *et.al* [17] using Adomian decomposition method and Optimal homotopy asymptotic method. Hydromagnetic flow of an Oldroyd-B fluid near an infinite plate induced by half rectified sine pulses using operational method has been analysed by Ghosh *et.al* [18]. Unsteady MHD thin film flow of an Oldroyd-B fluid over an oscillating inclined belt has been investigated by Gul *et.al* [19]. Uddin *et.al* [20] have constructed the similarity and analytical solutions of free convective flow of dilatant nanofluid in a Darcian porous medium with multiple convective boundary conditions. Choudhury and Dey [21] have constructed the closed form solutions of free convective elastico-viscous fluid flow past an inclined plate in slip flow regime using perturbation technique.

The objective of the present study is to investigate the effects of relaxation and retardation parameters on hydro-magnetic thin film flow consisting of nano-sized particles in an inclined belt in presence of convection-conduction and convection-diffusion phenomena.

## 2. MATHEMATICAL FORMULATION

The time-dependent thin film flow of Oldroyd-B nanofluid through an inclined belt with convective boundary condition at the upper surface is considered. The lower surface of the belt is oscillating about a non-zero mean velocity  $U$ . The motion of the fluid layer is in downward direction due to the influence of gravitational force  $g$ . Let  $x'$  axis be taken along the length of belt (infinite in length) and  $y'$  axis be taken perpendicular to it. The following assumptions are being made for studying the governing fluid motion:

- (i) Magnetic field ( $\vec{B}$ ) is applied along the transverse direction to the surface. Gauss's law of magnetism:  $\nabla \cdot \vec{B} = 0 \Rightarrow \vec{B} = B_0$ , i.e the strength of magnetic field is uniform.
- (ii) Magnetic Reynolds number is very small for weakly conducting system, so induced magnetic field may be neglected.
- (iii) As the speed of visco-elastic fluid flow is small, so energy dissipation due to viscosity may be neglected.
- (iv) Electric field intensity may be neglected in comparison to the Lorentz force.
- (v) Pressure is taken as uniform in the governing fluid motion, so pressure gradient is neglected.
- (vi) As the plate is infinite in length, fluidic properties like velocity, temperature and concentration are functions of  $y$  and  $t$  only.
- (vii) The pressure-diffusion in mass transfer is neglected because of zero pressure gradient.
- (viii) Temperature and concentration of fluid are assumed to be oscillating with time  $t$  about non-zero mean temperature and concentration respectively.
- (ix) At the outer edge of the belt, rate of deformation ( $\frac{\partial u}{\partial y}$ ) is taken as zero.
- (x) Outer surface is experienced by convection-diffusion and convection-conduction boundary conditions.

With these above assumptions, the equations of governing fluid motion are as follows:

Momentum equation:

$$\rho \left[ \frac{\partial u'}{\partial t'} + \lambda_1 \frac{\partial^2 u'}{\partial t'^2} \right] = \mu \left[ \frac{\partial^2 u'}{\partial y'^2} + \lambda_2 \frac{\partial^3 u'}{\partial y'^2 \partial t'} \right] - \left[ 1 + \lambda_1 \frac{\partial}{\partial t'} \right] \sigma B_0^2 u' + \rho g \sin \gamma \quad (2.1)$$

Energy equation:

$$\frac{\partial T'}{\partial t'} = \alpha \frac{\partial^2 T'}{\partial y'^2} + \beta D_B \frac{\partial T'}{\partial y'} \frac{\partial C'}{\partial y'} \quad (2.2)$$

Energy equation for species concentration:

$$\frac{\partial C'}{\partial t'} = D_B \frac{\partial^2 C'}{\partial y'^2} \quad (2.3)$$

The corresponding boundary conditions are as follows:

$$\begin{aligned} y' = 0 ; u' &= U + \epsilon U e^{i\omega' t'} ; T' = T_s + \epsilon (T_0 + T_s) e^{i\omega' t'} ; C' = C_s + \epsilon (C_0 + C_s) e^{i\omega' t'} ; \\ y' = 1 ; \frac{\partial u'}{\partial y'} &= 0 ; \frac{\partial T'}{\partial y'} = -\frac{h_f}{k} (T_s - T') ; \frac{\partial C'}{\partial y'} = -\frac{h_m}{D_b} (C_s - C') \end{aligned}$$

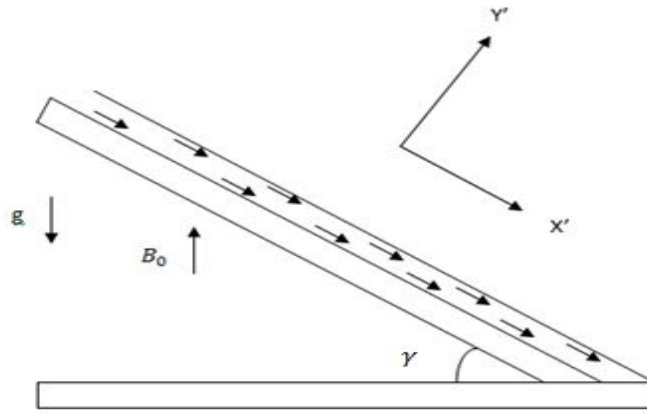


**Figure-1:** Geometry of the problem

### 3. METHOD OF SOLUTION

We introduce the following non-dimensional quantities to make the equations (2.1) to (2.3) dimensionless:

$$y = \frac{y'}{\delta}; u = \frac{u'}{U}; t = \frac{\mu t'}{\rho \delta}; \theta = \frac{T' - T_S}{T_0 - T_S}; \phi = \frac{C' - C_S}{C_0 - C_S}; a = \frac{\lambda_1 \mu}{\rho \delta^2}; b = \frac{\lambda_2 \mu}{\rho \delta^2}; M = \frac{\sigma B_0^2 \delta^2}{\mu}; \omega = \frac{\omega' \rho \delta^2}{\mu};$$

$$m = \frac{\rho \delta^2 g \sin \gamma}{\mu U}; Sc = \frac{\mu}{\rho D_b}; Pr = \frac{\mu}{\rho \alpha}; N_b = \frac{\rho^2 D_b (C_0 - C_S)}{\mu (T_0 - T_S)}$$

The dimensionless equations are as follows:

$$\frac{\partial u}{\partial t} + a \frac{\partial^2 u}{\partial t^2} = \frac{\partial^2 u}{\partial y^2} + b \frac{\partial^3 u}{\partial y^2 \partial t} - \left[ 1 + a \frac{\partial}{\partial t} \right] Mu + m \quad (3.1)$$

$$\frac{\partial \theta}{\partial t} = \frac{1}{Pr} \frac{\partial^2 \theta}{\partial y^2} + N_b \frac{\partial \theta}{\partial y} \frac{\partial \phi}{\partial y} \quad (3.2)$$

$$Sc \frac{\partial \phi}{\partial t} = \frac{\partial^2 \phi}{\partial y^2} \quad (3.3)$$

We use the following boundary conditions for solving the equations (3.1) and (3.3):

$$y = 0, u = 1 + \epsilon e^{i\omega t}, \theta = \epsilon e^{i\omega t}, \phi = \epsilon e^{i\omega t} \text{ \& } y = 1, \frac{\partial u}{\partial y} = 0, \theta = \frac{\delta h_f}{k} = Nc, \phi = \frac{\delta h_m}{D_b} = Nd \quad (3.4)$$

We use the perturbation technique to solve the equations (3.1) to (3.3). The velocity, temperature and concentration are taken as follows:

$$u = f_0 + \epsilon e^{i\omega t} f_1 + o(\epsilon^2), \theta = g_0 + \epsilon e^{i\omega t} g_1 + o(\epsilon^2), \phi = h_0 + \epsilon e^{i\omega t} h_1 + o(\epsilon^2) \quad (3.5)$$

Using (3.5) in the above equations (3.1) to (3.3), and comparing the co-efficient of  $\epsilon$ , we get

$$f_0'' - Mf_0 + m = 0 \quad (3.6)$$

$$f_1'' - (A_3 + iA_4)f_1 = 0 \quad (3.7)$$

$$\frac{1}{Pr} g_0'' + N_b g_0' h_0' = 0 \quad (3.8)$$

$$\frac{1}{Pr} g_1'' + N_b (g_1' h_0' + g_0' h_1') = i\omega g_1 \quad (3.9)$$

$$h_0'' = 0 \quad (3.10)$$

$$h_1'' = iSc\omega h_1 \quad (3.11)$$

Here we use the following boundary conditions:

$$y = 0; f_0 = 1; f_1 = 1; g_0 = 0; g_1 = 1; h_0 = 0; h_1 = 1 \text{ \& } y = 1; \frac{\partial f_0}{\partial y} = 0; \frac{\partial f_1}{\partial y} = 0; g_0 = \frac{\delta h_f}{k}; g_1 = 0; h_0 = \frac{\delta h_m}{D_b}; h_1 = 0 \quad (3.12)$$

### 4. RESULTS AND DISCUSSIONS

Solving the equations (3.6) to (3.11) and using the boundary conditions (3.12) we get the velocity profile, temperature and concentration as:

$$u = \frac{m}{M} + A_{11} \left( e^{\sqrt{M}y} + e^{\sqrt{M}(2-y)} \right) + \epsilon [\cos \omega t \{ e^{A_5 y} (A_7 \cos A_6 y - A_8 \sin A_6 y) + e^{-A_5 y} (A_9 \cos A_6 y + A_{10} \sin A_6 y) \} - \sin \omega t \{ e^{A_5 y} (A_8 \cos A_6 y + A_7 \sin A_6 y) + e^{-A_5 y} (A_{10} \cos A_6 y - A_9 \sin A_6 y) \} ] \quad (4.1)$$

$$\theta = \frac{\delta h_f}{k(1 - e^{A_{21}y})} (1 - e^{A_{21}y}) + \epsilon \cos \omega t [C_7 e^{A_{25}y} \cos A_{26}y + C_8 e^{A_{27}y} \cos A_{26}y + A_{32} e^{(A_{21}+A_{20})y} - A_{33} e^{(A_{21}-A_{20})y}] \quad (4.2)$$

$$\phi = \frac{\delta h_m}{D_b} + \epsilon [\cos \omega t \cos A_{20}y \{ A_{16} e^{A_{20}y} + A_{18} e^{-A_{20}y} \} + \cos \omega t \sin A_{20}y \{ A_{19} e^{A_{20}y} - A_{17} e^{-A_{20}y} \} - \sin \omega t \cos A_{20}y \{ A_{17} e^{A_{20}y} + A_{19} e^{-A_{20}y} \} - \sin \omega t \sin A_{20}y \{ A_{16} e^{A_{20}y} - A_{18} e^{-A_{20}y} \}] \quad (4.3)$$

The constants  $A_i$ 's ( $i=1, 2, \dots, 33$ ) are not presented here for the sake of brevity.

Here the shearing stress is represented by the following first order differential equation,

$$\left( 1 + k_1 \frac{\partial}{\partial t} \right) \tau = \left( 1 + k_2 \frac{\partial}{\partial t} \right) \left( \frac{\partial u}{\partial y} \right) \quad (4.4)$$

where,  $\tau$  is the dimensionless shearing stress and is given by

$$\tau = \frac{\tau'}{\rho f_0^2}$$

By solving the differential equation (4.4) and using the condition  $\tau = 0$  at  $y = 0$ , we get the shearing stress as:

$$\tau = A_{14} + \frac{\epsilon}{1+k_1^2 \omega^2} [\sin(\beta_1 + \omega t) - i \cos(\beta_1 + \omega t)] \quad (4.5)$$

Figure 2 to 5 represent the velocity profiles against the displacement variable for various values of flow parameters involved in the solution. It is seen that during the growth of relaxation parameter, fluid motion slows down. Physically, it can be interpreted that increase in relaxation time parameter is directly proportional to the storage of energy and as a consequence, fluid flow experiences retarding trend (figure 2). Retardation time parameter (figure 3) is connected with time scale in creeping motion of visco-elastic fluid and increasing values of retardation parameter accelerate the fluid motion. Figures reveal that there is a deficit by 1.03% in fluid motion during 400% growth in relaxation time parameter and an increase by 1.03% during the growth in retardation parameter by 200%.

Application of transverse magnetic field generates a force field known as Lorentz force, the combination of Lorentz force and viscosity makes the system thicker and as a result speed slows down. This physical phenomenon is clearly seen in our result [figure 4]. During the growth of  $M$  (magnetic parameter) by 20% (from  $M=2$  to 2.4), there is a fall in magnitude of velocity by 15.39% (approximately). Increase in gravitational parameter raises the power of inertia force and as a result fluid is accelerated [figure 5].

Shearing stress or viscous drag formed at the lower surface against the time  $t$  is drawn for various values of flow parameters are shown by figures 6 to 8. It clarifies the periodical variation of shearing stress against time. Effect of relaxation parameter on shearing stress is given by figure 7. In the interval  $[0, 1]$ , drag force is reduced during the rise in relaxation parameter but the oscillating nature of flow pattern, an opposite phenomenon is noticed in the interval  $[1, 4]$ . In  $[0, 2]$ , shearing stress is enhanced by the increase of retardation parameter. Physically it can be interpreted that the presence of viscosity and retardation parameter of visco-elasticity boosts the magnitude of shearing stress [figure 7]. An opposite fact is experienced in the interval  $[2, 5]$  due to the oscillating nature of flow with time. There is a significant amount of enhancement in viscous drag during a slight change in magnetic parameter. It can be justified as that the combination of viscosity and Lorentz force raises the viscous drag [figure 8].

Concentration profile against the time  $t$  is represented by figures 9 and 10. Both the graphs are drawn for the time interval  $[0, 5]$ . It is observed that there is a uniform variation in concentration profile for various values of convection parameter for diffusion. The result can be interpreted as that convection parameter for diffusion increases the species concentration periodically with respect to time. Schmidt number characterizes the combined effect of momentum and mass diffusions. Growth in Schmidt number increases the species concentration periodically with respect to time [figure 10].

## 5. CONCLUSIONS

Some of the important points from the above investigation are concluded as follows:

- i. Growth in relaxation time parameter retards fluid motion.
- ii. Retardation time parameter gears up the fluid motion.
- iii. Magnetic parameter may stabilize the fluid flow by reducing the speed of motion.
- iv. There is reduction in shearing stress by 0.05% (approximately) during the rise in when relaxation parameter. by 133% and growth in 0.04% (approximately) during 100% growth in retardation parameter.
- v. Shearing stress increases by 0.20% (approximately) as magnetic parameter increases by 0.10%.

## 6. GRAPHS

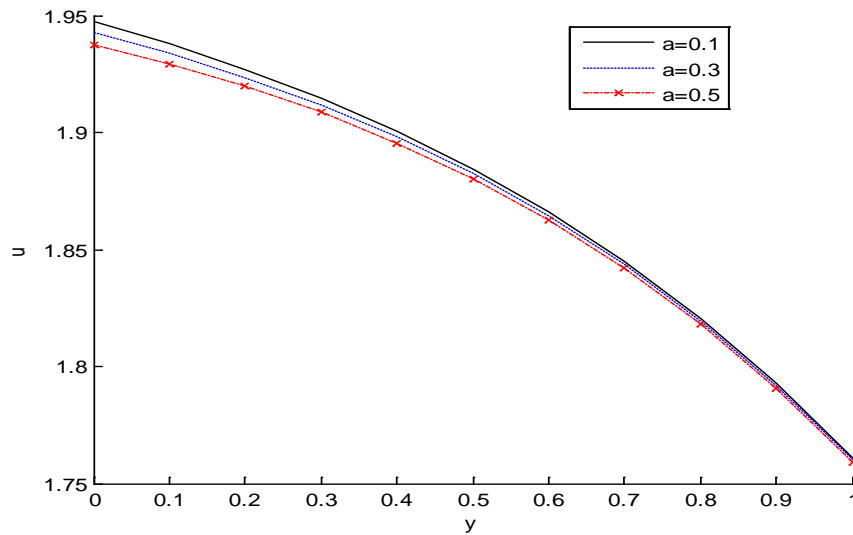


**Figure-2:** velocity  $u$  against  $y$  for  $b=0.3$ ,  $M=2$ ,  $Pr=4$ ,  $N_c=0.003$ ,  $N_b=0.05$ ,  $N_d=0.004$ ,  $m=4$ ,  $Sc=0.5$ ,  $\omega=1$ ,  $t=0.1$ ,  $\epsilon=0.01$ .

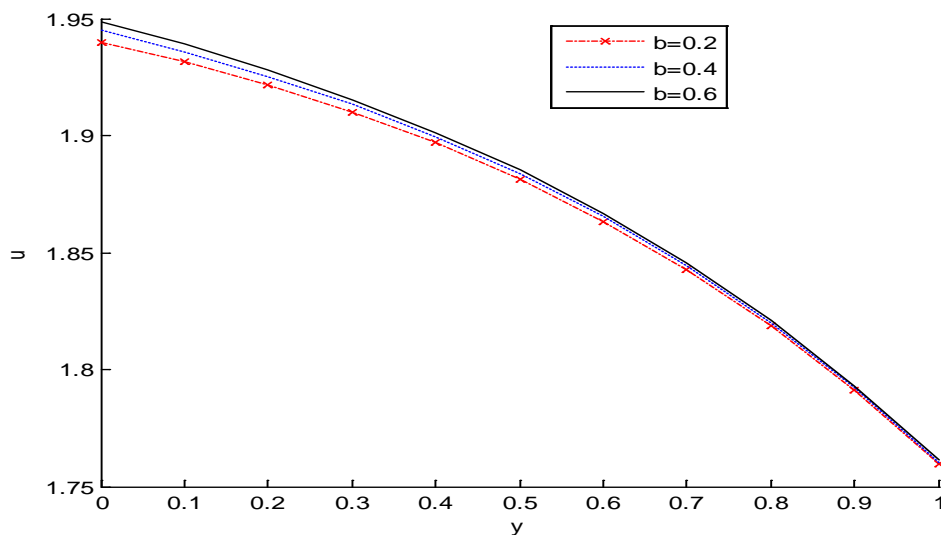


**Figure-3:** velocity  $u$  against  $y$  for  $a=0.3$ ,  $M=2$ ,  $Pr=4$ ,  $N_c=0.003$ ,  $N_b=0.05$ ,  $N_d=0.004$ ,  $m=4$ ,  $Sc=0.5$ ,  $\omega=1$ ,  $t=0.1$ ,  $\epsilon=0.01$ .

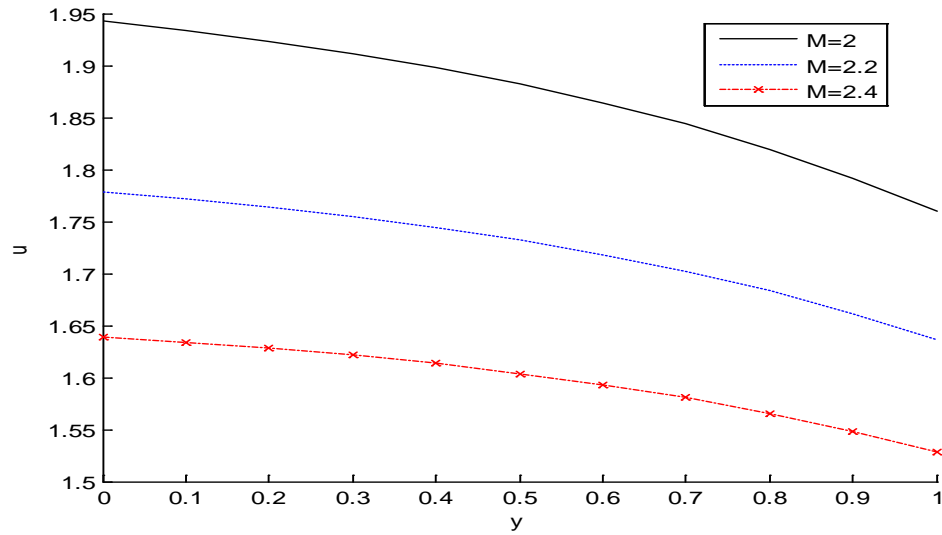


**Figure-4:** velocity  $u$  against  $y$  for  $a=0.3$ ,  $b=0.3$ ,  $Pr=4$ ,  $N_c=0.003$ ,  $N_b=0.05$ ,  $N_d=0.004$ ,  $m=4$ ,  $Sc=0.5$ ,  $\omega=1$ ,  $t=0.1$ ,  $\epsilon=0.01$ .

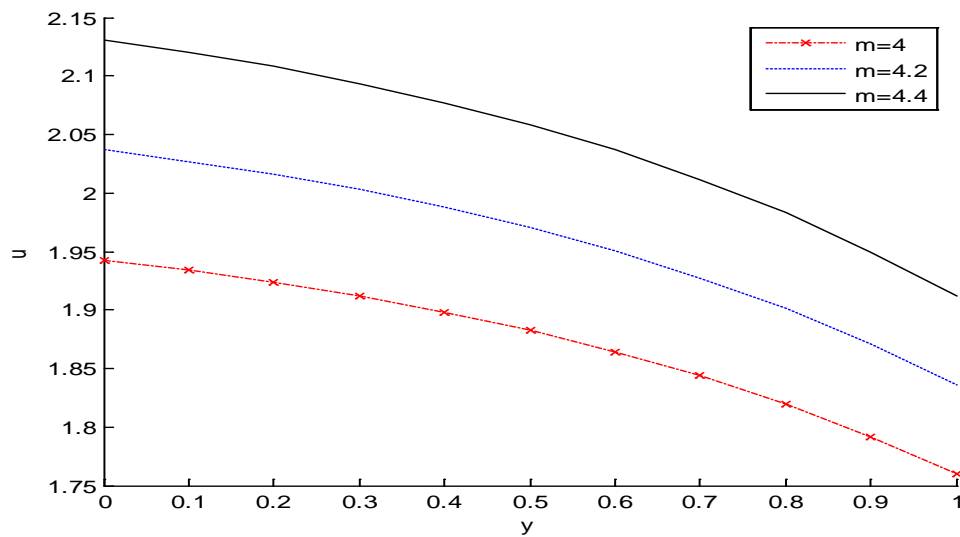


**Figure-5:** velocity  $u$  against  $y$  for  $a=0.3$ ,  $b=0.3$ ,  $M=2$ ,  $Pr=4$ ,  $N_c=0.003$ ,  $N_b=0.05$ ,  $N_d=0.004$ ,  $Sc=0.5$ ,  $\omega=1$ ,  $t=0.1$ ,  $\epsilon=0.01$ .

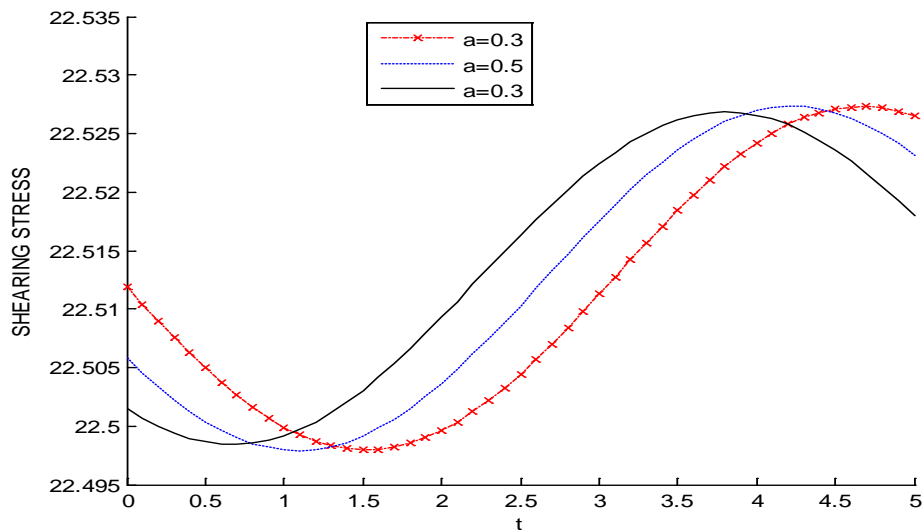


**Figure-6:** Shearing stress against  $t$  for  $b=0.3$ ,  $M=2$ ,  $Pr=4$ ,  $N_c=0.003$ ,  $N_b=0.05$ ,  $N_d=0.004$ ,  $m=4$ ,  $Sc=0.5$ ,  $\omega=1$ ,  $\epsilon=0.01$ ,  $y=0.4$ .

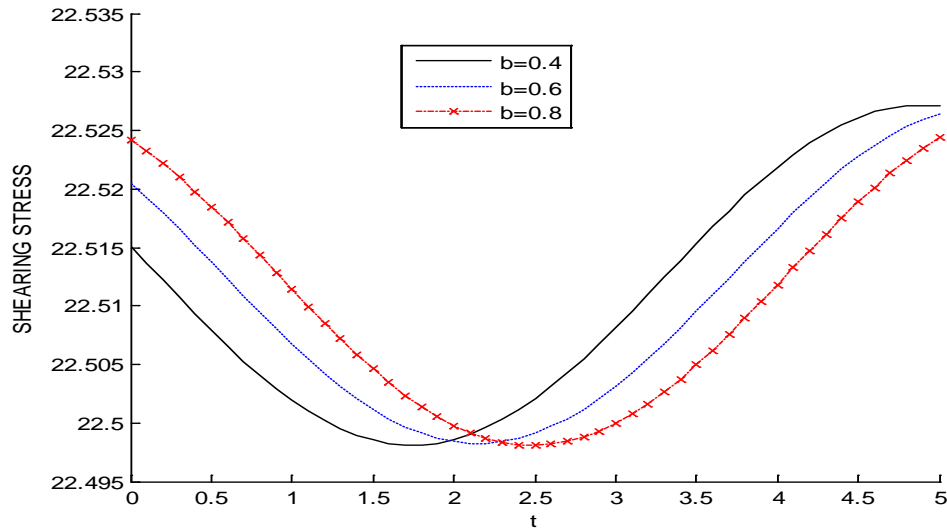


**Figure-7:** Shearing stress against  $t$  for  $a=0.3$ ,  $M=2$ ,  $Pr=4$ ,  $N_c=0.003$ ,  $N_b=0.05$ ,  $N_d=0.004$ ,  $m=4$ ,  $Sc=0.5$ ,  $\omega=1$ ,  $\epsilon=0.01$ ,  $y=0.4$ .

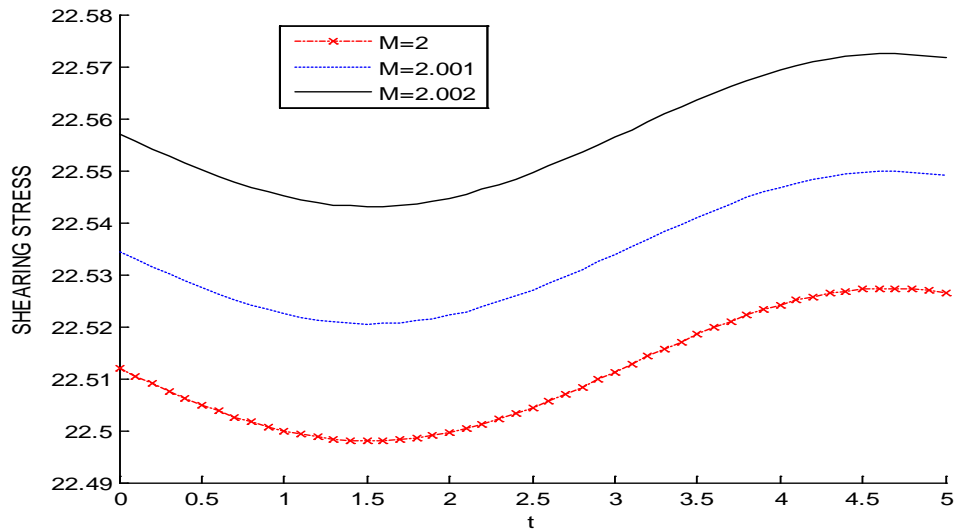


**Figure-8:** Shearing stress against  $t$  for  $a=0.3$ ,  $b=0.3$ ,  $Pr=4$ ,  $N_c=0.003$ ,  $N_b=0.05$ ,  $N_d=0.004$ ,  $m=4$ ,  $Sc=0.5$ ,  $\omega=1$ ,  $\epsilon=0.01$ ,  $y=0.4$ .

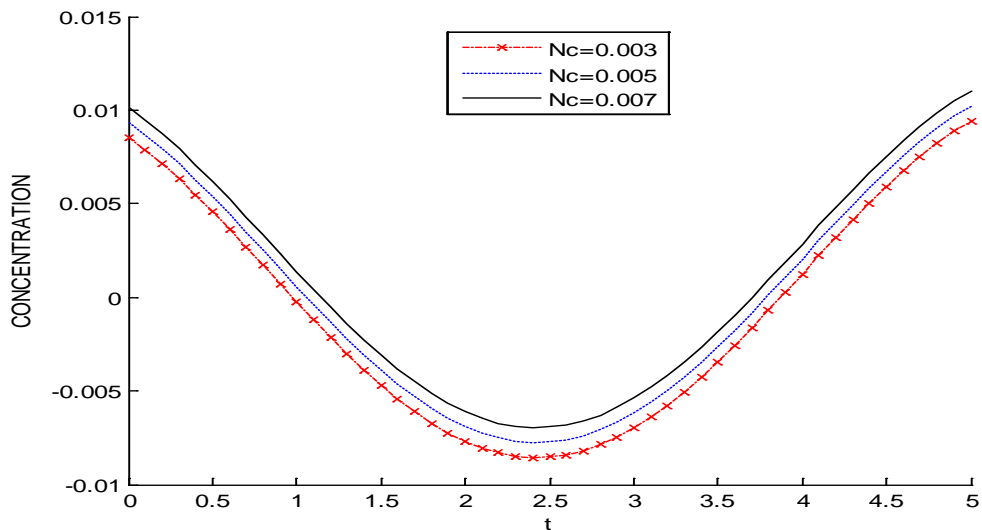


**Figure-9:** Concentration  $C$  against  $t$  for  $a=0.3$ ,  $b=0.3$ ,  $M=2$ ,  $Pr=4$ ,  $N_b=0.05$ ,  $N_d=0.004$ ,  $m=4$ ,  $Sc=0.5$ ,  $\omega=1$ ,  $\epsilon=0.01$ ,  $y=0.4$ .

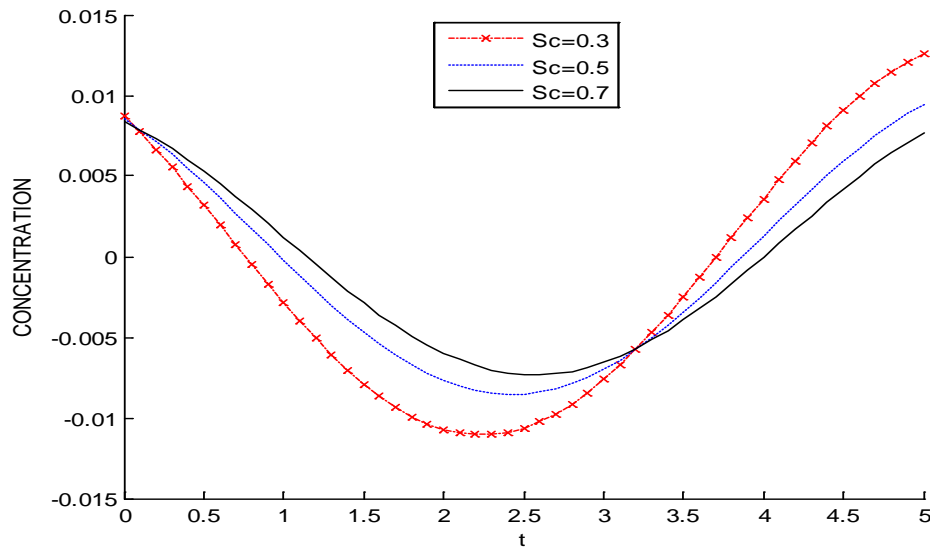


**Figure-10:** Concentration  $C$  against  $t$  for  $a=0.3$ ,  $b=0.3$ ,  $M=2$ ,  $Pr=4$ ,  $N_c=0.003$ ,  $N_b=0.05$ ,  $N_d=0.004$ ,  $m=4$ ,  $\omega=1$ ,  $\epsilon=0.01$ ,  $y=0.4$ .

## 7. REFERENCES

1. J. G. Oldroyd, On the formulation of rheological equations of state, *Proc. R. Soc. A* 200, (1950), 523–541.
2. J. G. Oldroyd, Non-Newtonian effects in steady motion of some idealized elastico-viscous liquids, *Proc. R. Soc. A* 245 (1958) 278–297.
3. D. Dey, Dusty Hydromagnetic Oldroyd Fluid Flow in a Horizontal Channel with Volume Fraction and Energy Dissipation, *International Journal of Heat and Technology*, 34(3) (2016) 415–422.
4. D. Dey, Hydromagnetic Oldroyd Fluid Flow Past A Flat Surface With Density And Electrical Conductivity, *Latin American Applied Research*, 47(2) (2017) 41–45.
5. D. Dey, Visco-elastic fluid flow through an annulus with relaxation, retardation effects and external heat source/sink, *Alexandria Engineering Journal*, (2017), DOI: <https://doi.org/10.1016/j.aej.2017.01.039>.
6. D. Dey and A. S. Khound, Relaxation and Retardation Effects on Free Convective Visco-elastic Fluid Flow past an Oscillating Plate, *International Journal of Computer Applications*, 144( 9) (2016) 34–40.
7. D. Dey and A. S. Khound, Hall Current Effects On Binary Mixture Flow Of Oldroyd-B Fluid Through A Porous Channel, *International Journal Of Heat And Technology*, 34(4) (2016) 687–693.
8. Hemorheology, Wikipedia. <[#Blood\\_viscoelasticity](https://en.wikipedia.org/wiki/Hemorheology)> (accessed 22 August 2017).
9. K. V. Wong and O.D. Leon, Applications of Nanofluids: Current and Future, *Advances in Mechanical Engineering*, 2010 (2010), Article ID 519659, 11 pages doi:10.1155/2010/519659.
10. A. K. Singh and C. K. Dikshit, Hydromagnetic flow past a continuously moving semi-infinite plate for large suction, *Astrophys. Space Sci.*, 148 (1988) 249–256.
11. D. A. Nield and A. V. Kuznetsov, The Cheng–Minkowycz problem for natural convective boundary-layer flow in a porous medium saturated by a nanofluid, *Int. J. Heat Mass Transf.*, 52 (2009) 5792–5795.
12. A. V. Kuznetsov and D. A. Nield, Thermal instability in a porous medium layer saturated by a nanofluid: Brinkman model, *Transp. Porous Media*, 81 (2010) 409–422.
13. A. Chamkha, R. S. R. Gorla and K. Ghodeswar, Non-similar solution for natural convective boundary layer flow over a sphere embedded in a porous medium saturated with a nanofluid, *Transp. Porous Media*, 86 (2010) 13–22.
14. R. A. Shah, S. Islam, M. Zeb, and I. Ali, Optimal homotopy asymptotic method for thin film flows of a third grade fluid, *Journal of Advanced Research in Scientific Computing*, 3(2) (2011) 1–14.
15. C. Y. Cheng, Natural convection boundary layer flow over a truncated cone in a porous medium saturated by a nanofluid, *International Communication in Heat and Mass Transfer*, 39 (2012) 231–235.
16. N. Shahid, M. Rana, and I. Siddique, Exact solution for motion of an Oldroyd-B fluid over an infinite flat plate that applies an oscillating shear stress to the fluid, *Boundary Value Problems*, 48 (2012) 1–19.
17. T. Gul, R. A. Shah, S. Islam and M. Arif, MHD Thin film flows of a third grade fluid on a vertical belt with slip boundary conditions, *J Appl Mathematics*, (2013) 1–14.
18. A. K. Ghosh, S. K. Datta, and P. Sen, A note on hydromagnetic flow of an Oldroyd-B fluid near an infinite plate induced by half rectified sine pulses, *Open Journal of Fluid Dynamics* 4 (2014) 226–240.
19. T. Gul, S. Islam, R. A. Shah, A. Khalid, I. Khan and S. Shafie, Unsteady MHD thin film flow of an Oldroyd-B fluid over an oscillating inclined belt, *PLOS*, (2015) 1–18.



20. M. J. Uddin, , B. Rostami, M. M. Rashid and P. Rostami, Similarity and analytical solutions of free convective flow of dilatant nanofluid in a Darcian porous medium with multiple convective boundary conditions, Alexandria Engineering Journal, 55 (2016) 263–274.
21. R. Choudhury and D. Dey, Free Convective Elastico-Viscous Fluid Flow With Heat And Mass Transfer Past An Inclined Plate In Slip Flow Regime, Latin American Applied Research, 42(4) (2012) 327-332.

## 8. NOMENCLATURE

$h_f$  heat transfer coefficient.  
 $K$  thermal conductivity.  
 $h_m$  mass transfer coefficient.  
 $N_c$  convection parameter for diffusion.  
 $N_d$  convection parameter for conduction.  
 $D_b$  diffusion coefficient.  
 $M$  magnetic parameter.  
 $m$  gravitational parameter.  
 $Sc$  Schmidt number,  $Pr$  Prandtl number.  
 $N_b$  Brownian motion parameter.  
 $u'$  velocity of fluid.  
 $y'$  displacement variable.  
 $t'$  time.  
 $T'$  temperature of fluid.  
 $C'$  concentration of nano-sized particle.  
 $y$  dimensionless displacement variable.  
 $u$  dimensionless velocity of fluid.  
 $t$  dimensionless time.  
 $T_0$  mean temperature.  
 $T_s$  temperature of fluid at static case.  
 $C_0$  mean concentration.  
 $C_s$  concentration of fluid at static case.  
 $Sh$  dimensionless shearing stress.  
 $a$  dimensionless relaxation time.  
 $b$  dimensionless retardation time.  
 $g$  gravitational constant.  
Greek Symbols:  
 $\rho$  density of the fluid.  
 $\delta$  thickness of the liquid layer.  
 $\alpha$  thermal diffusivity.  
 $\beta$  the ratio of effective heat capacity of the nano-particle and heat capacity of the fluid.  
 $\theta$  dimensionless temperature of fluid.  
 $\phi$  dimensionless concentration of nano-sized particle.  
 $\nu$  Kinematic viscosity.  
 $\omega'$  frequency of oscillation.  
 $\omega$  dimensionless frequency.  
 $\gamma$  angle made by the belt with the horizontal.

**Source of support: Nil, Conflict of interest: None Declared.**

**[Copy right © 2018. This is an Open Access article distributed under the terms of the International Journal of Mathematical Archive (IJMA), which permits unrestricted use, distribution, and reproduction in any medium, provided the original work is properly cited.]**